JOURNAL OF GUIDANCE, CONTROL, AND DYNAMICS
Vol. 15, No. 5, September-October 1992

Aerospace Plane Guidance Using Time-Scale Decomposition and Feedback Linearization

Mark A. Van Buren and Kenneth D. Mease
Princeton University, Princeton, New Jersey 08544

Single-stage vehicles using air-breathing propulsion hold promise for more economical delivery of payloads to orbit. Feedback guidance logic is developed for steering and accelerating such a vehicle along the super- and hypersonic segments of a near-minimum-fuel ascent trajectory. Accurate solutions of the minimum-fuel ascent problem show the effects of dynamic pressure, acceleration, and heating constraints and establish a basis for the development and assessment of guidance logic. The two-time-scale behavior in the optimal solution allows the state space to be decomposed into a control-dependent slow manifold and a family of fast manifolds. Near-optimal guidance is obtained by constructing a composite control law from the control for flying the minimum-fuel reduced-order trajectory on the slow manifold and a control for tracking the optimal reduced-order trajectory. The tracking problem is solved as a family of regulation problems corresponding to the family of fast manifolds, using the feedback linearization methodology from nonlinear geometric control theory. A complete characterization is given of all state transformation-static feedback pairs that lead to exact linearization of the fast dynamics. Simulation shows that the composite control law produces a near-minimum-fuel ascent.

Introduction

THE term "aerospace plane" is used in this paper to refer to a class of horizontal takeoff single-stage-to-orbit vehicles, distinguished by the use of primarily air-breathing engines to accelerate to orbital velocity. The anticipated advantages of such a vehicle are the operational flexibility of horizontal takeoff, the operational simplicity of a single stage, and the propellant mass reduction that results from using air-breathing engines. The effective use of air-breathing engines leads to lower altitude ascent trajectories compared to those of the Space Shuttles. Higher dynamic pressures, higher skin surface temperatures, and higher acceleration loads result.[1] The aerospace plane presents a challenging problem for guidance logic development. The guidance logic should lead to near-minimum-fuel orbit insertion, while ensuring that the vehicle does not transgress its flight envelope as defined by a set of prescribed constraints on dynamic pressure, acceleration, and heating.

This paper documents the development and evaluation of a concept for guiding the ascent of an aerospace plane through the atmosphere and into orbit. Our objective is to develop feedback guidance logic that leads to near-minimum-fuel ascent without violating any state or control constraints and that has modest computational requirements that are within the capabilities of an onboard computer. Only the super- and hypersonic segments of the atmospheric trajectory are considered, employing the point mass equations of motion in the vertical plane. We assume that the full state is available for feedback and do not directly address the issue of robustness.

We begin by formulating the minimum-fuel ascent problem and describing the aerodynamic and propulsion models for the aerospace plane that are used to obtain quantitative results. By use of a numerical optimization procedure, the ascent trajectories that minimize the propellant mass required to achieve orbit, while not violating vehicle dynamic pressure, acceleration, and heating constraints, are characterized. Benchmark mini-

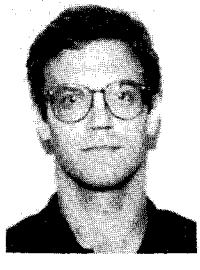

Mark A. Van Buren received his Masters in Aerospace Engineering from Delft University of Technology in 1987. He received his Ph.D. in Mechanical and Aerospace Engineering at Princeton University in June 1992. His research interests include flight mechanics, astrodynamics, and nonlinear dynamical control systems.

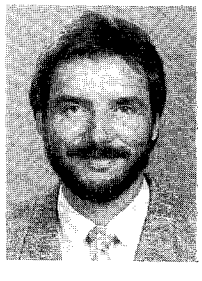

Kenneth D. Mease is an Assistant Professor of Mechanical and Aerospace Engineering at Princeton University. He received his B.S. degree from the University of Michigan and his M.S. and Ph.D. degrees from the University of Southern California. He worked previously in the Navigation Systems Section of the Jet Propulsion Laboratory. His research centers on the application of optimal and nonlinear control theories, perturbation methods, and dynamical systems theory to aerospace vehicle trajectory design, guidance, navigation, and control. He received the Princeton University School of Engineering Emerson Electric Award (1989) for research and teaching. He is an Associate Editor for the *Journal of Guidance, Control, and Dynamics* and an Associate Fellow of the AIAA.

Received March 27, 1991; revision received Aug. 5, 1991; accepted for publication Oct. 2, 1991.

mum-fuel ascent trajectories for increasingly restrictive constraints are obtained, and their salient features are described.

We approach the guidance problem from a geometric perspective.[2,3] Because of the two-time-scale nature of the dynamics, we view the state space as being composed of a control-dependent slow manifold and a family of fast manifolds. Figure 1 illustrates the geometric two-time-scale decomposition viewpoint. A feedback control is derived by separately designing a slow control for the dynamics on the slow manifold and a fast control for the dynamics on the fast manifolds and then combining them.

The slow control is designed by solving the minimum-fuel ascent problem on the slow manifold. The resulting optimal trajectory on the slow manifold is an approximation to the minimum-fuel trajectory obtained in the complete state space using the full-order dynamics. An exact decomposition of the dynamics cannot be obtained; thus, an asymptotic expansion in the time-scale ratio is employed to determine an approximate slow manifold. The optimal reduced-order solution on the approximate slow manifold is compared to the benchmark trajectories and is shown to be an accurate approximation. Moreover, the procedure for determining the reduced-order minimum-fuel trajectory and controls is greatly simplified compared to that for the full-order problem and would probably be suitable for onboard real-time guidance. Composite feedback control based on a zeroth-order approximation to the slow manifold leads to a good approximation of the minimum-fuel ascent trajectory but requires relatively high gains in the fast feedback controller. An improved first-order approximation to the slow manifold is shown to yield accurate guidance with moderate fast feedback gains.

Stabilization of the dynamics along the fast manifold is achieved by applying linear state feedback to the *exactly* linearized fast dynamics. A complete characterization of the nonlinear state transformation-static feedback pairs that exactly linearize the nonlinear dynamics on the family of fast manifolds is obtained, independent of the order of the slow manifold approximation.

There have been numerous applications of the two-time-scale approach to flight mechanics problems.[4,5] The first application of this approach to the aerospace plane ascent optimization and guidance problem was by Corban et al.[6,7] Their analysis of the reduced-order minimum-fuel solution on the slow manifold has provided considerable insight into the features of the optimal solution. Sauvageot et al.[8] have utilized a similar approach for the aerospace plane ascent problem. In neither case were the time-scale decompositions validated by comparison of the solutions with accurate solutions for the full-order problem. We provide evidence that the time-scale decomposition proposed by Corban et al. is valid. Regarding the design of the fast control, Corban et al. have considered the optimal control problem on the fast manifold and shown that the optimal control (in this case the lift) cannot be obtained in state feedback form. They then used a particular state transformation-static feedback pair to exactly linearize the dynamics on the fast manifold and subsequently designed a regulator via pole placement. We take a more general approach to the feedback linearization of the dynamics on the fast manifold and, as a result, identify all state transformation-static feedback pairs that lead to exact linearization. This added flexibility proves useful in developing a simplified, potentially more robust, near-optimal guidance concept.

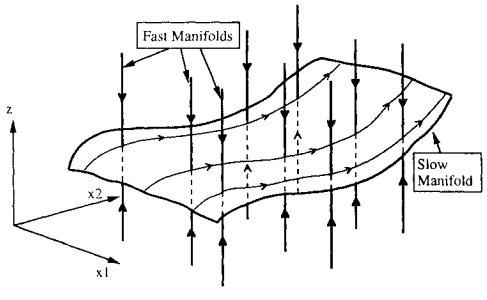

Fig. 1 Schematic representation of the geometry of the transversal intersection of the fast and slow manifolds in 4D state space.

The natural combination of two-time-scale decomposition and feedback linearization methodologies has been applied to other flight mechanics problems by Menon et al.,[9] Snell et al.,[10] and Singh.[11] Meyer et al.[12] and Lane and Stengel[13] applied feedback linearization to the aircraft rigid-body dynamics.

Aerospace Plane Model

Equations of Motion

The translational motion of the vehicle mass center is assumed to be governed by the dynamic equations for flight over a spherical (R_E), homogeneous, nonrotating Earth. The gravitational acceleration is given by the inverse square law $g = \mu/r^2$. Furthermore, the ascent trajectory is confined to a great circle plane; that is, the heading is fixed and the bank angle is not a control variable. The equations are[14]

$$\frac{dV}{dt} = \frac{T\cos\alpha - D}{m} - \frac{\mu}{r^2}\sin\gamma \tag{1a}$$

$$\frac{d\gamma}{dt} = \frac{L + T\sin\alpha}{mV} - \left(\frac{\mu}{r^2} - \frac{V^2}{r}\right)\frac{\cos\gamma}{V} \tag{1b}$$

$$\frac{dr}{dt} = V\sin\gamma \tag{1c}$$

$$\frac{dm}{dt} = -\frac{T}{g_E I_{sp}} \tag{1d}$$

where, as usual, $L = C_L q S_{ref}$ and $D = C_D q S_{ref}$, with $q = \frac{1}{2}\rho V^2$, the dynamic pressure. The atmospheric density ρ is a function of the altitude $h = r - R_E$. The propulsive force and specific impulse are given by

$$T(V, h, \eta_{ab}, \eta_r) = \eta_{ab} T_{max_{ab}}(V, h) + \eta_r T_{max_r} \tag{2a}$$

$$I_{sp}(V, h, \eta_{ab}, \eta_r) = I_{sp_{ab}}(V, h) I_{sp_r} \frac{\eta_{ab} T_{max_{ab}}(V, h) + \eta_r T_{max_r}}{\eta_{ab} T_{max_{ab}}(V, h) I_{sp_r} + \eta_r T_{max_r} I_{sp_{ab}}(V, h)} \tag{2b}$$

where η_{ab} and η_r are the throttles for the air-breathing engine and the rocket engine, respectively. A throttleable rocket is necessary for maneuvering outside the atmosphere and can also be used to provide thrust in the higher regions of the atmosphere. Note that the specific impulse of each individual propulsion mode is assumed not to be affected by throttling of the corresponding engine.

Vehicle Modeling

The gross takeoff weight is estimated to be 300,000 lbf, of which ~60% is fuel. The overall length of the vehicle is 233.4 ft, and its aerodynamic reference area is 6000 ft^2. Trimmed values for the overall lift coefficient C_L and drag coefficient C_D as functions of Mach number M and angle of attack α are obtained from an available hypersonic vehicle model.[15]

The air-breathing engine for an aerospace plane is expected to be capable of several distinct propulsion modes, each suited to operate over a specific speed range. Our propulsion model consists of a ramjet with either subsonic or supersonic combustion. The air-breathing modes are mutually exclusive. The model, based on a one-dimensional thermodynamic analysis, provides maximum thrust $T_{max_{ab}}$ and the corresponding fuel specific impulse $I_{sp_{ab}}$.[16]

Minimum-Fuel Ascent to Orbit

The minimum-fuel ascent problem is to determine the trajectory and required control histories that lead to a specified low Earth orbit, not to violate the state and control constraints, and maximize the mass inserted into orbit. The controls are the throttle settings η_{ab} and η_r and the lift L (or, equivalently, the angle of attack α).

Initial and Final Conditions

The minimum-fuel ascent is assumed to commence after an initial climbout and acceleration phase. The initial point of the minimum-fuel ascent coincides with the switch to the ramjet propulsion mode. The mode switch is estimated to occur at $M_i = 3.0$ and a commensurate altitude, determined by the initial dynamic pressure $q_i = 2{,}000$ lbf/ft^2. The mass at the end of the initial climbout m_i is assumed to be 8703 slug ($W_i = 280{,}000$ lbf). The initial flight-path angle γ_i is taken to be zero.

The final conditions are determined by the requirement that the vehicle is to be inserted into a circular low Earth orbit (LEO) beyond the sensible atmosphere. The radius defining the boundary of the sensible atmosphere R_A should be large enough that the burnout conditions are reached before exiting the atmosphere. In that case, the motion beyond the sensible atmosphere will be Keplerian.

After exiting the atmosphere, the vehicle must be on an elliptical transfer orbit with apogee distance r_{LEO}, the altitude of the target low Earth orbit, to minimize fuel consumption.[17] This imposes a final condition on the state at the edge of $r_e = R_A$:

$$\frac{V_e}{V_{LEO}} = \kappa \sqrt{\frac{2(\kappa - 1)}{\kappa^2 - \cos^2 \gamma_e}} \tag{3}$$

where V_{LEO} is the circular speed in the final low Earth orbit, and $\kappa = r_{LEO}/r_e > 1$.

Performance Index

Minimum-fuel trajectories are determined by maximizing the mass inserted into a circular orbit at r_{LEO}:

$$J = m_{LEO} = m_e \exp\left(\frac{V_a - V_{LEO}}{g_o I_{sp_r}}\right) \tag{4}$$

where $V_a = (1/\kappa) V_e \cos \gamma_e$ is the velocity at the apogee of the transfer orbit.

State and Control Constraints

The ascent to orbit using air-breathing propulsion is confined to a severely restrictive ascent corridor determined by heating, structural, aerodynamic, and acceleration constraints. A detailed knowledge of the vehicle is required to specify the constraints precisely. For our purposes the following constraints are used. The dynamic pressure is limited by

$$q = \tfrac{1}{2}\rho V^2 \le q_{max} \tag{5}$$

The axial and normal load factors in the body axes system are limited by

$$a = \frac{T - R\cos(\alpha + \delta)}{m g_o} \le a_{max} \tag{6a}$$

$$n = \frac{R \sin(\alpha + \delta)}{m g_o} \le n_{max} \tag{6b}$$

where $R = \sqrt{L^2 + D^2}$ is the resultant aerodynamic force, and $\tan \delta = L/D$. The approximate stagnation point convective heating rate is limited by

$$Q = K\sqrt{\rho}\, V^3 \le Q_{max} \tag{7}$$

Optimal Trajectories and Controls

The trajectory optimization problem is (approximately) solved using the Optimal Trajectories by Implicit Simulation (OTIS)[18] computer program. The approach on which OTIS is based is to formulate the optimal control problem as a constrained nonlinear programming problem using implicit integration of the trajectory by a collocation method. The states along the trajectory as well as the controls are represented by cubic splines. The appeal of this approach lies in that it can readily accommodate state and control constraints.

Numerical solutions are obtained for a circular target low Earth orbit at an altitude of 100 n.mi. with the sensible atmosphere reaching to an altitude of 354,000 ft and conforming to the U.S. 1976 Standard Atmosphere. The corridor constraints are $q_{max} = 2000$ lbf/ft^2 and $Q_{max} = 400$ Btu/ft^2/s. The maximum sustainable axial load is put at $\pm 1 g_o$. The maximum normal load is set to be $\pm 3 g_o$. The constant of proportionality in Eq. (7) is taken to be $K = 2.058 \cdot 10^8$, with Q in Btu/ft^2/s, ρ in slug/ft^3, and V in ft/s.

The three optimal ascent trajectories shown in Fig. 2 illustrate the effects of the constraints. The first trajectory is subject to a dynamic pressure constraint ($q \le 2000$ lbf/ft^2) only. Note that the optimal trajectory in this case consists of tracking the dynamic pressure constraint up to final climbout. The second trajectory shows the effect of introducing an additional constraint on the axial load factor ($a \le 1 g_o$). The ascent is flown at full throttle. Adjustment of the thrust level to meet the axial load constraint is achieved by using lift to increase the altitude above that imposed by the dynamic pressure constraint. The final trajectory reflects the effect of the addition of a heating rate constraint ($Q \le 400$ Btu/ft^2/s). Note that the optimal trajectory at high speeds is off the dynamic pressure constraint boundary and on the heating rate constraint boundary.

Guidance Law Design

Two-Time-Scale Decomposition of State Space and Composite Control

The aim of a two-time-scale decomposition of the state space into slow and fast modes is to allow separate (and simplified) design of feedback controllers for the respective modes, which can then be combined to form a composite feedback controller for the full-order dynamics. The two-time-scale decomposition is predicated on identifying small terms in the equations of motion, which are subsequently parameterized by the scalar ϵ, $0 \le \epsilon \ll 1$, representing the ratio of speeds of the slow and fast modes ($\epsilon = t/\tau$).

Transformation to the Standard Two-Time-Scale Model

Corban et al.[6,7] have proposed a two-time-scale decomposition of the ascent trajectory dynamics in which the classical energy state approach[4,5] is modified to account for the changing mass. Their method is based on the observation that for the aerospace plane both the fuel flow and axial load factor are relatively small. After introduction of the additional simplification that the thrust is aligned with the velocity, the dynamics are brought into their standard singular perturba-

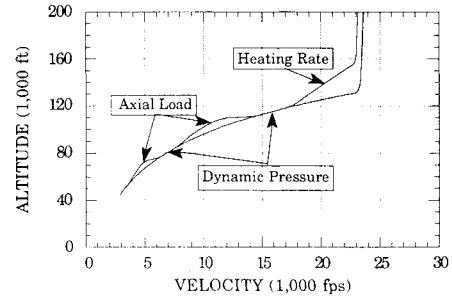

Fig. 2 Full-order optimal ascent trajectories.

tion form on the slow time scale ($t = \epsilon\tau$) through the definition of the specific energy $E = V^2/2 - \mu/r$ and the state transformation $(V, m, r, \gamma)^T \rightarrow (E, m, r, \gamma)^T$. Note that thrust-velocity alignment is only introduced to simplify the presentation; subsequent developments can be readily carried out for the more general case.[7,16]

$$\left.\begin{aligned} \frac{dE}{dt} &= \frac{V[T - D(L)]}{m} \\ \frac{dm}{dt} &= -\frac{T}{g_E I_{sp}} \end{aligned}\right\} \quad \frac{dx}{dt} = f(x, z, u) \quad (8a)$$

$$\left.\begin{aligned} \epsilon\frac{dr}{dt} &= V \sin\gamma \\ \epsilon\frac{d\gamma}{dt} &= \frac{L}{mV} - \left(\frac{\mu}{r^2} - \frac{V^2}{r}\right)\frac{\cos\gamma}{V} \end{aligned}\right\} \quad \epsilon\frac{dz}{dt} = g(x, z, u) \quad (8b)$$

where V is now viewed as a function of E and r, and $u = (L, \eta_{ab}, \eta_r)^T$. The presence of ϵ suggests that the rates of change of r and γ are much faster than those of E and m (by a factor of $1/\epsilon$). As $\epsilon \rightarrow 0$ the rates of change of r and γ tend to infinity, when viewed on the slow time scale, unless $g = 0$, whereas the rates of change of E and m remain finite. Viewed on the fast time scale, using $d/d\tau = \epsilon(d/dt)$, the rates of change of E and m tend to zero as $\epsilon \rightarrow 0$, whereas the rates of change of r and γ remain finite. The system dynamics clearly evolve on two separate time scales for $\epsilon \ll 1$; i.e., the equations of motion are in the form of a two-time-scale system and as such are amenable to the aforementioned composite feedback design approach.

Geometric Characterization of the Two-Time-Scale Decomposition

A two-time-scale decomposition is geometrically characterized by the existence for $\epsilon = 0$ of an isolated smooth control-dependent slow (or equilibrium) manifold and a family of smooth control-independent fast (or conservation) manifolds that are transverse to the slow manifold.[19]

In the limiting case $\epsilon = 0$, r and γ equilibrate instantaneously in response to changes in E, m, and the control L, if viewed on the slow time scale t. In this case, for a given feedback control function $L(x, z)$, the trajectory evolves on a 2D slow (or equilibrium) manifold $\mathcal{S}_o^L$ defined by

$$\mathcal{S}_o^L = \left\{(E, m, r, \gamma): V \sin\gamma = 0 \;\&\; \frac{L}{mV} - \left(\frac{\mu}{r^2} - \frac{V^2}{r}\right)\frac{\cos\gamma}{V} = 0\right\} \quad (9)$$

where the superscript L indicates the dependence on the lift control. As a result, on a slow manifold γ and L can be expressed in terms of E, m, and r. Specifically,

$$\gamma_o = 0 \quad (10a)$$

$$L_o = m_o\left(\frac{\mu}{r_o^2} - \frac{V^2(E_o, r_o)}{r_o}\right) \quad (10b)$$

where the subscript o indicates the value on the slow manifold for $\epsilon = 0$. In other words, flight at any point on $\mathcal{S}_o^L$ is level with force equilibrium normal to the flight path. Substituting the expression for L_o into Eq. (8a), one obtains a second-order dynamic system that dictates the evolution of E and m on $\mathcal{S}_o^L$, with r treated as a control (replacing L) in addition to η_{ab} and η_r. [Equivalently, one could solve Eq. (10b) for r_o, substitute the result into Eq. (8a), and obtain a second-order system for E and m with η_{ab}, η_r, and L as the controls. However, this approach is not as convenient for carrying out the subsequent calculations.]

In the limiting case $\epsilon = 0$, and viewed on the fast time scale, the energy and mass are constant and the dynamics of r and γ evolve on a 2D fast (or conservation) manifold (a plane):

$$\mathcal{F}^{E_o, m_o} = \{(E, m, r, \gamma): E = E_o \;\&\; m = m_o\} \quad (11)$$

The condition that the family of fast manifolds is transversal to the slow manifold allows for a local decomposition of the state space into fast and slow modes, along the respective manifolds. It has been verified[16] that $\mathcal{S}_o^L$ and $\mathcal{F}^{E_o, m_o}$ are indeed transversal at any point $(E_o, m_o, r_o, \gamma_o)$ whenever

$$\frac{\partial L}{\partial r} < m_o\frac{V(E_o, r_o)^2}{r_o^2} \quad \text{and} \quad \frac{\partial L}{\partial \gamma} < 0$$

In the case $\epsilon \neq 0$, it can be shown that for small enough ϵ the geometry of the two-time-scale decomposition is preserved.[3] The slow manifold $\mathcal{S}_\epsilon^L$ is an invariant manifold: once the state is on it, the state remains on it. This requires the z evolution along the slow manifold to match the z dynamics. Let the slow manifold for $\epsilon \neq 0$ be described by

$$z = s[x, u_s(x, \epsilon), \epsilon] \quad (12)$$

The manifold condition, matching the z dynamics to the z evolution, is

$$\epsilon\frac{dz}{dt} = \epsilon\left(\frac{\partial s}{\partial x} + \frac{\partial s}{\partial u_s}\frac{\partial u_s}{\partial x}\right) f[x, s(x, u_s, \epsilon), u_s] = g[x, s(x, u_s, \epsilon), u_s] \quad (13)$$

After introducing the "true" fast variable $\eta = z - s(x, u_s, \epsilon)$, the system dynamics can be rewritten as

$$\frac{dx}{dt} = f[x, s(x, u_s, \epsilon) + \eta, u] \quad (14a)$$

$$\epsilon\frac{d\eta}{dt} = g[x, s(x, u_s, \epsilon) + \eta, u] - g[x, s(x, u_s, \epsilon), u_s] - \epsilon\left(\frac{\partial s}{\partial x} + \frac{\partial s}{\partial u_s}\frac{\partial u_s}{\partial x}\right)\{f[x, s(x, u_s, \epsilon) + \eta, u] - f[x, s(x, u_s, \epsilon), u_s]\} \quad (14b)$$

where $u = u_s + \Delta u$, and $\Delta u = 0$ along the slow manifold. Note that in terms of x and η, the slow manifold is described as $\eta = 0$.

Composite Feedback Control

For sufficiently small ϵ the dynamic behavior of the system is characterized by rapid motion along the fast manifolds, involving η, combined with a more leisurely slide along the slow manifold, involving x. This two-time-scale decomposition permits the use of a composite feedback control of the form

$$u = u_s(x) + u_f^x(\eta) \quad \text{and} \quad u_f^x(0) = 0 \quad (15)$$

where the slow and fast feedback control can be designed separately. When the fast dynamics are stable, or stabilized by feedback, η will rapidly approach zero; i.e., the state will rapidly approach the slow manifold. In that case the slow dynamics can be adequately modeled as

$$\frac{dx}{dt} = f[x, s(x, u_s, \epsilon), u_s] \quad (16)$$

discarding any influence of the fast variables on the slow dynamics. Likewise, it is convenient to approximate the fast dynamics by only retaining the dominant, i.e., $\mathcal{O}(\epsilon^0)$, contribution:

$$\frac{d\eta}{d\tau} = g\{x, s[x, u_s(x), \epsilon] + \eta, u_s(x) + u_f^x(\eta)\} - g\{x, s[x, u_s(x), \epsilon], u_s(x)\} \tag{17}$$

Employing the composite feedback control of the form of Eq. (15) renders the slow manifold Eq. (12) a function of the slow state x only: $s[x, u_s(x, \epsilon), \epsilon] = s(x, \epsilon)$. Obtaining a closed-form solution for s from the manifold condition will generally be impossible. Instead, the graph s of the slow manifold and the slow component of the control u_s are approximated by truncated asymptotic series in ϵ:

$$s[x, u_s(x, \epsilon), \epsilon] = s_o(x) + \epsilon s_1(x) + \epsilon^2 s_2(x) + \cdots \tag{18a}$$

$$u_s(x, \epsilon) = u_o(x) + \epsilon u_1(x) + \epsilon^2 u_2(x) + \cdots \tag{18b}$$

Substituting these power series in the manifold condition and equating like powers in ϵ, one obtains, to first order in ϵ,

$$0 = g(x, s_o, u_o) \tag{19a}$$

$$\frac{ds_o}{dx} f(x, s_o, u_o) = \frac{\partial g}{\partial z}\bigg|_{S_o^{u_o}} s_1 + \frac{\partial g}{\partial u}\bigg|_{S_o^{u_o}} u_1 \tag{19b}$$

which are solved for the zeroth and first-order terms, respectively. Satisfying the manifold condition to higher order in ϵ enables one to refine the approximation for $s(x, \epsilon)$ and $u_s(x, \epsilon)$ to any order.[2,3]

Composite feedback control is applied to the ascent trajectory guidance through the decomposition of the lift feedback:

$$L = L_s(E, m) + L_f^{E,m}(\Delta r, \Delta\gamma), \qquad L_f^{E,m}(0, 0) = 0 \tag{20}$$

where $\Delta r = r - r_s$ and $\Delta\gamma = \gamma - \gamma_s$. E and m appear as parameters in the fast feedback control. The design task of the slow controller $L_s(E, m)$ is to control the slow dynamics along the slow manifold [Eq. (16)] to minimize fuel consumption. The task of the fast controller is to ensure the time-scale separation and render the slow manifold asymptotically stable. The throttle settings η_{ab} and η_r do not appear in the fast dynamics due to the thrust-velocity alignment assumption. Hence, both η_{ab} and η_r only have a slow component; the optimization along the slow manifold completely determines the throttle settings. The composite control achieves near-optimal performance up to the terminal climbout phase. Guidance for the terminal phase is not considered in this paper.

Minimum-Fuel Slow Control

Our purposes in this section are to determine the minimum-fuel trajectory and controls on the slow manifold, which will be referred to as the reduced-order solution, compare them with the results obtained for the full-state optimization, and thereby assess the validity of the time-scale decomposition and the composite control design methodology.

Zeroth-Order Slow Control

By changing the independent variable from time to mass (which is strictly monotonically *decreasing* under the reasonable assumption that no coasting occurs during the ascent), application of the minimum principle can be shown to lead to the following control logic for minimizing the fuel consumption:

$$r_o, \eta_{ab_o}, \eta_{r_o} = \arg\max_{r, \eta_{ab}, \eta_r} \left\{ \frac{V[T - D(L)]}{m} \frac{g_E I_{sp}}{T} \right\} \tag{21}$$

at each point (E, m) along the reduced-order optimal trajectory, where the lift is specified by Eq. (10b).

Since the throttles appear linearly in the slow dynamics, the throttle logic will be bang-bang. The optimal throttle logic in the unconstrained case is

$$\begin{aligned}
&\text{(I)} && I_{sp_{ab}} \geq I_{sp_r} && \eta_{ab_o} = 1 \\
&\text{(Ia)} && EI_{sp_{ab}} \geq I_{sp_r} && \eta_{r_o} = 0 \\
&\text{(Ib)} && EI_{sp_{ab}} < I_{sp_r} && \eta_{r_o} = 1 \\
&\text{(II)} && I_{sp_r} > I_{sp_{ab}} && \eta_{r_o} = 1 \\
&\text{(IIa)} && EI_{sp_r} \geq I_{sp_{ab}} && \eta_{ab_o} = 0 \\
&\text{(IIb)} && EI_{sp_r} < I_{sp_{ab}} && \eta_{ab_o} = 1
\end{aligned} \tag{22}$$

where $EI_{sp} = [(T_{max} - D)/T_{max}]I_{sp}$ is the effective specific impulse. The completely singular case, i.e., the case where both η_{ab} and η_r are allowed to take on intermediate values, can be ruled out under the assumption that $I_{sp_r} > 0$. Moreover, it can be shown, using the generalized Legendre-Clebsch condition that the partially singular case, i.e., the case where only the secondary throttle is allowed to take on intermediate values, is nonoptimal. Case (I), where the specific impulse of the air breather is higher than the rocket I_{sp}, is the case of primary interest. Conditions (Ia) and (Ib) are a consequence of the fact that it is optimal to use the rocket to provide additional thrust only if the total effective specific impulse will be increased by doing so. The optimal altitude r_o is subsequently determined from Eq. (21) using the appropriate throttle settings and the restriction

$$R_E \leq r_o \leq r_{max} = \min(-\mu/E, R_A)$$

The introduction of a dynamic pressure constraint and a stagnation-point heating rate constraint leads to an implicit lower bound on the altitude. This is because, for fixed E, both q and Q are functions of altitude only. Observe that the throttle switching logic is unaffected by the presence of either a dynamic pressure or a heating rate constraint.

The introduction of an axial load constraint may in principle lead to an optimal throttle setting at intermediate values whenever the constraint is active. However, we have found that for maximum thrust levels up to 2.5 times the ones used in this paper, fuel optimal flight along the axial load constraint is achieved at full throttle.

The global altitude optimization consists of a coarse search over the permissible altitude range, as determined by the constraints, to bracket candidate maxima, followed by a local gradient ascent. Comparison of the local maxima determines the globally optimizing altitude.

The throttle switching logic [Eq. (22)] agrees with that derived by Corban et al.[7] in their common domain of applicability; it includes the situation in which the air breather has become less efficient than the rocket, but considers a less complicated propulsion model.

First-Order Slow Control

Clearly, whenever r_o is not constant, the approximation $\gamma_o = 0$ is not a good one. A better estimate of the flight-path angle can be obtained by including the first-order correction as computed from the manifold condition. Equation (20b) leads to

$$\frac{\partial r_o}{\partial E}\frac{dE_o}{dt} + \frac{\partial r_o}{\partial m}\frac{dm_o}{dt} = V_o\gamma_1 \tag{23a}$$

and

$$L_1 = m(V_o^2/r_o^2)r_1 \tag{23b}$$

Observe that Eq. (23b) corresponds to the first variation of Eq. (10b), identifying L_1 with δL_o and r_1 with δr_o (note that this is generally not the case). Now take into consideration that the zeroth-order *optimization* implies that, to first order, no performance gains can be obtained by perturbing r from r_o when r and L are related by Eq. (10b). Since the first-order corrections r_1 and L_1 coincide with the first variations of r_o and L_o, they must necessarily be zero: $r_1 = L_1 = 0$. Hence, the first-order approximation to the slow manifold is $r_s = r_o$ and $\gamma_s = \gamma_1$. The first-order approximate slow control is $L_s = L_o$. The partial differentials in Eq. (23a) necessary to evaluate γ_1 are determined by finite differencing.

Corban et al.[7] have obtained results similar to ours, including the use of a flight-path-angle correction, to improve the accuracy of the reduced solution. Here we have shown this improvement to result from the systematic development of a first-order approximation to the slow manifold.

Numerical Validation of Decomposition Geometry

The validity of the time-scale decomposition has been assessed by a direct comparison of the optimal trajectories on the slow manifold with the corresponding optimal trajectories obtained using OTIS. In Fig. 3 a (first-order) slow manifold approximation is plotted beside its counterpart computed with OTIS. All three constraints are enforced along both trajectories. Observe the excellent agreement between the two trajectories, apart from the terminal phase. Further study of the terminal phase is warranted. In particular, it is of interest to adequately incorporate the final conditions leading to insertion into orbit.

Stabilizing Fast Control

To obtain a fast control law that is optimal and stabilizing (i.e., that forces the fast state to the reduced solution), one may try to solve the optimization problem for the family of fast manifolds that arises from a formal boundary-layer analysis. This approach has been pursued in Refs. 6, 7, and 20. However, it has been shown that this does not lead to a control law in feedback form.

An alternative approach is to design a nonoptimal feedback control law that will stabilize the fast dynamics. The control law must generate a flow on the fast manifold so that the intersection of the slow manifold (2D) and the appropriate fast manifold (2D) is an asymptotically stable equilibrium point, for $\epsilon = 0$ (see Fig. 1). In that case, the slow manifold will be a stable manifold for small enough ϵ. If the fast dynamics are truly fast, any stabilizing control law will be near-optimal, since most of the flow transversal to the fast manifolds will occur near the optimal reduced solution.

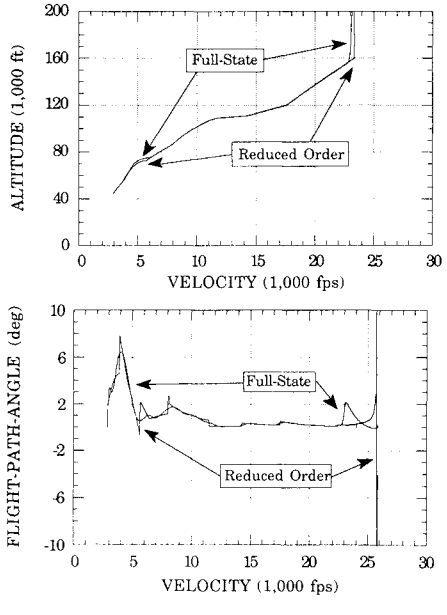

Fig. 3 Comparison of the reduced-order (slow) optimal ascent trajectory to the full-order optimal ascent trajectory.

The methodology followed here to obtain stabilizing feedback controllers is to exactly linearize the fast dynamics using feedback linearization and then to stabilize the linearized dynamics using linear (static) feedback. Full-state feedback is assumed.

Feedback Linearization of the Dynamics on the Fast Manifolds

The dynamics on the family of fast manifolds are described by a control-linear single-input system:

$$\frac{d\eta}{dt} = a(\eta) + b(\eta)u \tag{24}$$

with

$$a(\eta) = \begin{bmatrix} V\sin\gamma - V_s\sin\gamma_s \\ -\left(\frac{\mu}{r^2} - \frac{V^2}{r}\right)\frac{\cos\gamma}{V} - \frac{L_s}{mV_s} + \left(\frac{\mu}{r_s^2} - \frac{V_s^2}{r_s}\right)\frac{\cos\gamma_s}{V_s} \end{bmatrix}$$

$$b(\eta) = \begin{bmatrix} 0 \\ \frac{1}{mV} \end{bmatrix}, \qquad \eta = \begin{bmatrix} \Delta r \\ \Delta\gamma \end{bmatrix}, \tag{25}$$

$$u = L = L_s(E, m) + L_f^{E,m}(\Delta r, \Delta\gamma)$$

where $r = r_s + \Delta r$ and $\gamma = \gamma_s + \Delta\gamma$, and, as a matter of convenience, the total lift L has been designated as the control variable instead of, more formally, only its fast part $L_f^{E,m}$. The fast dynamics can be exactly linearized using a nonlinear coordinate transformation and nonlinear static feedback, if and only if there exists a (distinguished) output function $y = h(\eta)$ such that the system has relative degree $n = 2$ (see Isidori[21]). It can be readily verified that, for $\cos\gamma \neq 0$, any strictly monotonic function of Δr constitutes a distinguished output function and as such defines a nonlinear state transformation-static feedback pair that transforms the fast dynamics into its Brunovsky normal form: a second-order linear system with a double integrator open-loop transfer function.[16] A proportional-derivative (PD) controller $k_P(1 + k_D s)$ plus negative feedback can subsequently be applied for pole placement. The gains k_P and k_D can be selected to give satisfactory dynamic behavior on the fast manifolds. In particular, the fast dynamics should be asymptotically stable and truly fast compared to the slow dynamics.

For a given distinguished output $h(\Delta r)$ the linearizing feedback can be found by differentiating twice:

$$y = h(\Delta r)$$

$$\frac{dy}{d\tau} = \frac{\partial h}{\partial \Delta r}(V\sin\gamma - V_s\sin\gamma_s)$$

$$\frac{d^2y}{d\tau^2} = \frac{\partial^2 h}{\partial \Delta r^2}(V\sin\gamma - V_s\sin\gamma_s)^2 - \frac{\partial h}{\partial \Delta r}\frac{\mu}{Vr^2}(V\sin\gamma - V_s\sin\gamma_s)\sin\gamma + \frac{\partial h}{\partial \Delta r} \times \left[\frac{L}{mV} - \left(\frac{\mu}{r^2} - \frac{V^2}{r}\right)\frac{\cos\gamma}{V} - \frac{L_s}{mV_s} + \left(\frac{\mu}{r_s^2} - \frac{V_s^2}{r_s}\right)\frac{\cos\gamma_s}{V_s}\right]V\cos\gamma = \nu \tag{26}$$

and solving for the control L:

$$L = \frac{m}{\cos\gamma} \times \left[\left(\frac{\mu}{r^2} - \frac{V^2}{r} \right) \cos^2\gamma + \frac{\mu}{Vr^2} \times (V \sin\gamma - V_s \sin\gamma_s)\sin\gamma + \frac{L_s}{m}\frac{V}{V_s}\cos\gamma - \left(\frac{\mu}{r_s^2} - \frac{V_s^2}{r_s} \right) \frac{V}{V_s} \cos\gamma_s \cos\gamma - \frac{h^{(2)}}{h^{(1)}} \times (V \sin\gamma - V_s \sin\gamma_s)^2 + \frac{\nu}{h^{(1)}} \right] \tag{27}$$

where

$$h^{(1)} = \frac{\partial h}{\partial \Delta r} \quad \text{and} \quad h^{(2)} = \frac{\partial^2 h}{\partial \Delta r^2}$$

Clearly, L can be solved in terms of ν only if $(\cos\gamma)/m \neq 0$ and $h^{(1)} \neq 0$; i.e., h is a distinguished output. Note that the fast dynamics are feedback linearized without any assumptions regarding the accuracy of the slow manifold approximation.

Altitude Controller

An obvious choice for the distinguished output is the altitude $r = r_s + \Delta r$ itself.[7] In that case $h^{(1)} = 1$ and $h^{(2)} = 0$, and one obtains

$$L = \frac{m}{\cos\gamma} \times \left[\left(\frac{\mu}{r^2} - \frac{V^2}{r} \right) \cos^2\gamma + \frac{\mu}{Vr^2}(V\sin\gamma - V_s\sin\gamma_s) \times \sin\gamma + \frac{L_s}{m}\frac{V}{V_s}\cos\gamma - \left(\frac{\mu}{r_s^2} - \frac{V_s^2}{r_s} \right) \frac{V}{V_s} \cos\gamma_s \cos\gamma + k_p(r_s - r) + k_p k_D (V_s \sin\gamma_s - V \sin\gamma) \right] \tag{28}$$

Dynamic Pressure Controller

Alternatively, one may choose dynamic pressure as the distinguished output. Note that on the fast manifolds the dynamic pressure is a strictly decreasing function of the altitude only, when density is assumed to be a function of altitude only:

$$h(\Delta r) = q = \tfrac{1}{2}\rho V^2 = \rho(r)\left(E + \frac{\mu}{r} \right) \tag{29}$$

$$h^{(1)} = -\left(q\beta + \frac{\mu}{r^2}\rho \right)$$

$$h^{(2)} = \left[q\left(\beta^2 - \frac{d\beta}{dr} \right) + \frac{2\mu}{r^2}\rho\left(\frac{1}{r} + \beta \right) \right] \tag{30}$$

where $\beta = -(1/\rho)(d\rho/dr)$ is the inverse scale height for an exponential density approximation. Substitution into Eq. (27) leads to a nonlinear feedback control law that tracks the dynamic pressure along the slow manifold. When the reduced-order solution is on the dynamic pressure constraint, $q_s = q_{max}$, the dynamic pressure controller will have a constant reference signal.

Stagnation Point Heating Rate Controller

In a similar fashion, by observing that the approximation of the stagnation-point heating rate in Eq. (7) is also a strictly decreasing function of altitude only on the fast manifolds, one can obtain a linearization with Q as a distinguished output:

$$h(r) = Q = K\sqrt{\rho}V^3 = 2\sqrt{2}K\sqrt{\rho(r)}\left(E + \frac{\mu}{r} \right)^{3/2} \tag{31}$$

Level Axial Load Factor Controller

Another interesting alternative is the level axial load factor, defined as

$$a_L(r) = \left(\frac{T_{max} - D_{level}}{mg_o} \right) \tag{32}$$

where the drag is determined from the level flight condition. The axial load factor itself cannot be used as a distinguished output, since it contains the control L (as distinct from L_s, which is a function of E and m). The level axial load factor is, however, a function of the altitude only at each (E, m) pair. Furthermore, over the altitude range of interest, it is a strictly decreasing function of the altitude. The level axial load factor is a good approximation to the true axial load factor for small enough deviations from the slow manifold. It therefore seems reasonable to regulate the axial load factor via control of the level axial load factor.

Ascent Trajectory Guidance Using Composite Feedback Control

The guidance strategy is to compute the minimum-fuel control for the approximate reduced-order trajectory and the tracking control needed to drive the state to the optimal reduced-order trajectory at each guidance update and to use the sum of the two, the composite control, to command the throttle(s) and the lift. The computation of the optimal controls for the reduced-order trajectory requires parameter optimization to determine the optimal altitude and consequently the optimal lift.

If it can be assured a priori that the minimum-fuel ascent is along constraint boundaries, a simplified guidance strategy is possible. At each guidance update, the active constraint is determined, and the appropriate fast controller is used to compute the lift required to track the active constraint (boundary). The omission of the parameter optimization eliminates the possibility of optimal switching between the two combustion modes. The switch between the two modes occurs when their thrust levels are equal. Operationally this may be preferable to switching optimally, since it will eliminate discontinuity in acceleration. The thrust for the active mode is always at its maximum.

If the objective is to track constraint boundaries, it is reasonable to ask why the altitude controller is not used exclusively, instead of using the dynamic pressure controller to track the dynamic pressure boundary, etc. If one were merely interested in regulating the dynamics on the fast manifolds, all four controllers are equally well qualified (presuming the selection of stabilizing gains). In all four cases the state is driven to the point of intersection of the fast manifold with the optimal reduced-order trajectory on the slow manifold, the only difference being the shape of the transients for the state variables. Therefore, one might in that case choose the simplest controller, namely, the one for the altitude.

However, since the true motion is not confined to one particular fast manifold and one is really interested in tracking the reduced-order solution, there are potential advantages to the use of the alternative controllers. For an optimal ascent trajectory that entails climbing the active constraints in sequence, application of the dynamic pressure, heating rate, and axial load controllers, respectively, leads to a constant reference input for the constraint specific controller. In contrast, the altitude controller will have a time-varying reference input. Moreover, the accuracy with which the altitude controller tracks a particular constraint depends on the accuracy of the

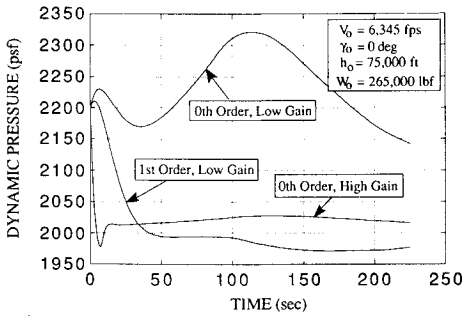

Fig. 4 Nonlinear dynamic pressure tracker.

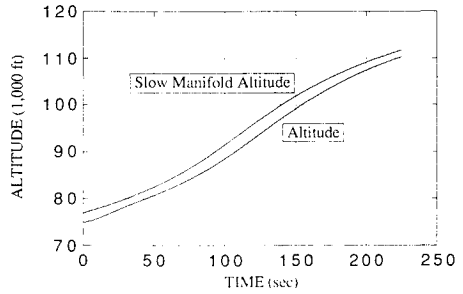

a) Zeroth-order approximation and low gains

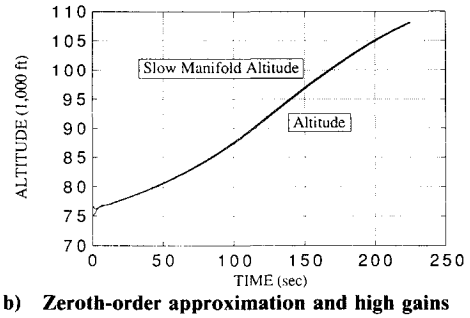

b) Zeroth-order approximation and high gains

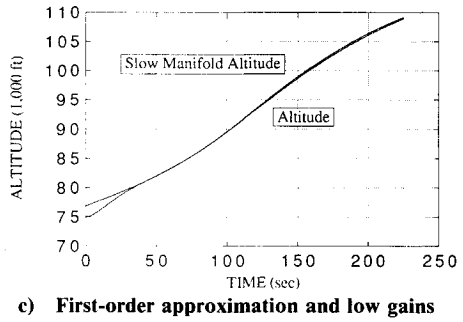

c) First-order approximation and low gains

Fig. 5 Tracking of the slow manifold.

model relating altitude to the constrained quantity. If the constrained quantities can be measured directly, use of the constraint controllers limits the disruptive effects of modeling errors. Another consequence of the indirect nature of the altitude controller in tracking the constraints and the nonlinearity of the problem is that a constant-gain altitude controller regulates the dynamic pressure with varying performance along the ascent trajectory. A dedicated constraint controller, on the other hand, will have uniform performance, i.e., it has automatic gain scheduling.

Nonlinear Dynamic Pressure Tracker

Figure 4 presents the responses to an initial error of $\sim 10\%$ in dynamic pressure, applying a zeroth-order dynamic pressure tracker with high and low gain, respectively, as well as a low-gain first-order one. It is clear that the zeroth-order low-gain dynamic pressure tracker ($\omega_n = 0.103$ rad/s, $\zeta = 0.780$) is not sufficient.

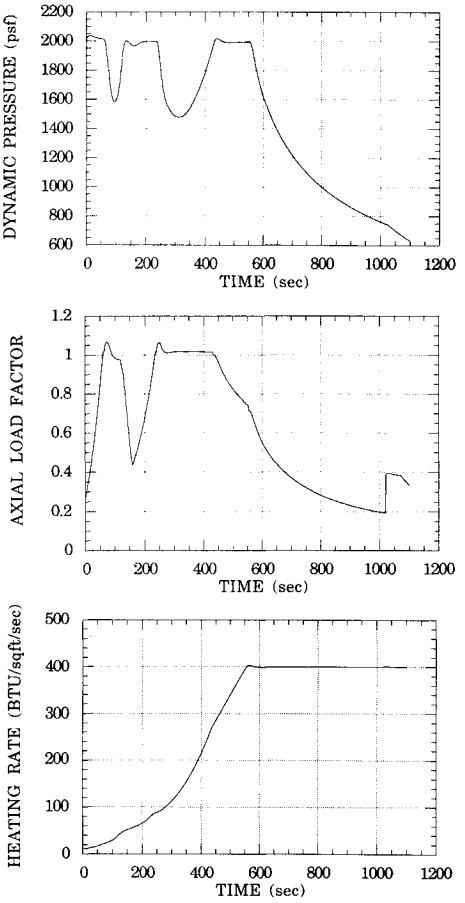

Fig. 6 Values of the constraint functions along the tracked ascent trajectory.

The poor performance in tracking the dynamic pressure is caused by inadequate tracking of the slow manifold (Fig. 5a), which is mainly due to inaccurate derivative information: $\gamma_o = 0$. Better tracking employing the zeroth-order slow manifold approximation can be obtained by increasing the gain ($\omega_n = 1.03$ rad/s, $\zeta = 0.780$). Clearly, the slow manifold is now closely tracked (Fig. 5b). A more desirable alternative is to apply the first-order slow manifold approximation with low gain; the response is less abrupt, and larger errors can be accommodated without running into control saturation. The first-order approximation leads to good tracking of the slow manifold with low gains (Fig. 5c).

Near-Minimum-Fuel Ascent by Constraint Tracking

The dynamic pressure, level axial load, and heating rate controllers are used to guide our aerospace plane model along the super- and hypersonic segments of an ascent trajectory. In Fig. 6, the values of the three distinguished outputs demonstrate the tracking effectiveness and illustrate the switching from one constraint boundary to the next. The guided trajectory is near-optimal: The performance of the constraint tracker, compared with the full-state (OTIS) trajectory in terms of fuel consumed up to the start of the terminal ascent phase ($M = 21$), is 133,921 lbf vs 132,908 lbf. This result can be improved by increasing the feedback gains of the fast controller. The computational requirements for constraint tracking are modest.

Conclusions

Numerical solutions of the minimum-fuel ascent problem have been presented to show the effects of dynamic pressure, acceleration, and heating constraints and to establish a basis for the development and assessment of guidance logic. For the vehicle and propulsion models used, the minimum-fuel strat-

egy is to fly along the most restrictive constraint boundary as energy is gained using air-breathing engines. The most restrictive constraint shifts from dynamic pressure to acceleration load to heating as the vehicle accelerates through the super- and hypersonic regimes.

We approached the guidance law design problem from a geometric perspective. After providing evidence of two-time-scale behavior in the optimal solution, we viewed the state space as being composed of a control-dependent slow manifold and a family of fast manifolds. Near-optimal guidance was obtained by constructing a composite control law from the control for flying the minimum-fuel reduced-order trajectory on the slow manifold and a control for tracking the optimal reduced-order trajectory. By employing asymptotic series to approximate the slow manifold and its associated slow control, the optimal controls for the slow trajectory were obtained in feedback form, except for the complication that a parameter optimization problem must be solved at each guidance cycle. Carrying out the asymptotic approximation to first order was shown to allow smaller gains in the tracking control. The tracking problem was solved as a family of regulation problems corresponding to the family of fast manifolds, using the feedback linearization methodology from nonlinear geometric control theory. It was shown that any strictly monotonic function of altitude can be used as a distinguished output and leads to a linearizing state transformation-static feedback pair. In particular, constraint trackers with automatic gain scheduling were derived.

Simulation results showed that the composite feedback guidance law generates a near minimum-fuel ascent trajectory for the super- and hypersonic segments. An even simpler strategy of using the nonlinear trackers to follow the active constraints was also shown to produce a near-optimal ascent for the particular vehicle model employed. Near-optimality was verified by direct comparison with an accurate minimum-fuel ascent trajectory that satisfies the specified orbit insertion conditions. The computational requirements for either scheme are modest and should be within the capabilities of the computers onboard an aerospace plane.

Acknowledgments

This research was supported by NASA Langley Research Center under Contract NAG-1-907. We thank the U.S. Air Force for making the OTIS computer program available.

References

[1]Schoettle, U. M., "Performance Analysis of Rocket-Ramjet Propelled SSTO Vehicles," 36th Congress of the International Astronautical Federation, Paper 85-133, Stockholm, Sweden, Oct. 1985.

[2]Kokotovic, P. V., "Recent Trends in Feedback Design: An Overview," *Automatica*, Vol. 21, No. 3, 1985, pp. 225–236.

[3]Kokotovic, P. V., Khalil, H. K., and O' Reilly, J., *Singular Perturbation Methods in Control: Analysis and Design,* Academic Press, New York, 1986.

[4]Rutowski, E. S., "Energy Approach to the General Aircraft Performance Problem," *Journal of the Aeronautical Sciences,* Vol. 21, No. 3, 1954, pp. 187–195.

[5]Bryson, A. E., Jr., Desai, M. N., and Hoffman, W. C., "Energy-State Approximation in Performance Optimization of Supersonic Aircraft," *Journal of Aircraft,* Vol. 6, No. 6, 1969, pp. 481–488.

[6]Corban, J. E., Calise, A. J., and Flandro, G. A., "Trajectory Optimization and Guidance Law Development for National Aerospace Plane Applications," *Proceedings of the 1988 American Control Conference,* Vol. 2, June 1988, pp. 1406–1411.

[7]Corban, J. E., Calise, A. J., and Flandro, G. A., "Rapid Near-Optimal Aerospace Plane Trajectory Generation and Guidance," *Journal of Guidance, Control, and Dynamics,* Vol. 14, No. 6, 1991, pp. 1181–1190.

[8]Sauvageot, A., Golan, O., and Breakwell, J., "Minimum Fuel Trajectory for the Aerospace-Plane," AAS/AIAA Astrodynamics Specialist Conference, Paper 89-0352, Stowe, VT, Aug. 1989.

[9]Menon, P. K. A., Badgett, M. E., Walker, R. A., and Duke, E. L., "Nonlinear Flight Test Trajectory Controllers for Aircraft," *Journal of Guidance, Control and Dynamics,* Vol. 10, No. 1, 1987, pp. 67–72.

[10]Snell, S. A., Enns, D. F., and Garrard, W. L., Jr., "Nonlinear Inversion Flight Control for a Supermaneuverable Aircraft," *Proceedings of the AIAA Guidance, Navigation, and Control Conference,* Vol. 1, AIAA, Washington, DC, 1990, pp. 808–817.

[11]Singh, S. N., "Control of Nearly Singular Decoupling Systems and Nonlinear Aircraft Maneuver," *IEEE Transactions on Aerospace and Electronic Systems,* Vol. 24, No. 6, Nov. 1988, pp. 775–784.

[12]Meyer, G., Su, R., and Hunt, R. L., "Application of Nonlinear Transformations to Automatic Flight Control," *Automatica,* Vol. 20, No. 1, 1984, pp. 103–107.

[13]Lane, S. H., and Stengel, R.F., "Flight Control Design Using Nonlinear Inverse Dynamics," *Automatica,* Vol. 24, No. 4, 1988, pp. 471–483.

[14]Miele, A., *Flight Mechanics: Theory of Flight Paths,* Addison-Wesley, Reading, MA, 1962.

[15]Shaughnessy, J. D., Pinckney, S. Z., McMinn, J. D., Cruz, C. I. and Kelley, M.-L., "Hypersonic Vehicle Simulation Model: Winged-Cone Configuration," NASA TM 102610, Langley, VA, Nov. 1990.

[16]Mease, K. D., and Van Buren, M. A., "Trajectory Optimization and Guidance for an Aerospace Plane," Final Rept. NASA Contract NAG-1-907, Princeton, NJ, Nov. 1990.

[17]Vinh, N. X., and Marchal, C., "Analytical Solutions of a Class of Optimum Orbit Modifications," *Journal of Optimization Theory and Applications,* Vol. 5, No. 3, 1970, pp. 178–196.

[18]Hargraves, C. R., and Paris, S. W., "Direct Trajectory Optimization Using Nonlinear Programming and Collocation," *Journal of Guidance, Control, and Dynamics,* Vol. 10, No. 4, 1987, pp. 338–342.

[19]Marino, R., and Kokotovic, P. V., "A Geometric Approach to Nonlinear Singularly Perturbed Control Systems," *Automatica,* Vol. 24, No. 1, 1988, pp. 31–41.

[20]Calise, A. J., and Corban, J. E., "Optimal Control of Singularly Perturbed Nonlinear Systems with State-Variable Inequality Constraints," *Proceedings of the AIAA Guidance, Navigation, and Control Conference,* Vol. 2, AIAA, Washington, DC, 1990, pp. 1226–1235.

[21]Isidori, A., *Nonlinear Control Systems, An Introduction,* 2nd ed., Springer-Verlag, New York, 1989.